Wan et al. BioMedical Engineering OnLine (2025) 24:42
https://doi.org/10.1186/s12938-025-01379-4

BioMedical Engineering OnLine

RESEARCH Open Access

Exploration of the effect of morphology and location on hemodynamics of small aneurysms: a variable-controlled study based on two cases with tandem aneurysms

Jun Wan[1,2†], Yeqing Jiang[3†], Ligang Xu[2], Qimin Zhang[4], Guanghu Xu[4], Long Yu[4], Xinzhuo Li[4], Xiaolong Zhang[3*] and Shengzhang Wang[1,4*]

†Jun Wan and Yeqing Jiang are first author.

*Correspondence: xiaolongzhang@fudan.edu.cn; szwang@fudan.edu.cn

[1] Academy for Engineering and Technology, Fudan University, Shanghai, China
[2] Department of Interventional Radiology, Jing'an District Central Hospital, Fudan University, Shanghai 200040, China
[3] Department of Radiology, Huashan Hospital Affiliated to Fudan University, 12 Wulumuqi Zhong Road, Shanghai 200040, China
[4] Department of Aeronautics and Astronautics, Institute of Biomechanics, Fudan University, No. 220 Handan Road, Shanghai 200433, China

Abstract

Introduction: Small aneurysms are usually treated with a flow diverter alone, without coils. However, some continue to exhibit incomplete occlusion after treatment, even after an extended period. This study aimed to investigate the effects of aneurysm morphology and location on the hemodynamic parameters related to poor outcomes.

Methods: Two patients with tandem aneurysms were enrolled. Flow diverter deployment was simulated, and preoperative and postoperative hemodynamics were analyzed using computational fluid dynamics. The preoperative and postoperative hemodynamics of the actual surgical plan were simulated using finite element analysis and computational fluid dynamics. The correlation between morphology, hemodynamics, and incomplete occlusion was evaluated by calculating the hemodynamics of aneurysm models with different heights and neck widths, adjusted according to the original geometry.

Results: Simulation of the actual surgical plan showed that the incompletely occluded aneurysm had a larger postoperative velocity at the sac and neck region (v_a and v_{neck}) and residual flow volume than the occluded aneurysm in both cases. The inflow rate (Q_{inflow}), inflow concentration index (ICI), v_a, and residual flow volume increased when the aneurysm neck width was expanded; with the increase in height, Q_{inflow} and ICI increased up to a certain point, while v_a and residual flow volume showed a decreasing trend. Aneurysms located on the superior wall of the internal carotid artery ophthalmic segment had a larger v_{neck} than those on the inferior wall.

Conclusion: Aneurysms located on the superior wall of the internal carotid artery ophthalmic segment or with a larger neck or height present a more severe hemodynamic environment, requiring careful consideration when planning surgery. This study provides hemodynamic evidence demonstrating how morphology affects aneurysm progression.

Keywords: Tandem aneurysms, Computational fluid dynamics, Flow diverter device, Tubridge, Computed fluid dynamic

Introduction

Subarachnoid hemorrhage (SAH), a type of hemorrhagic stroke, is characterized by high mortality. Its incidence rate in 2021 was 37.09% higher than that in 1990 [1]. The rupture of intracranial aneurysms (IAs) is one of the primary causes of subarachnoid hemorrhage. IAs occur in approximately 3–5% of the general population, with an annual rupture rate of approximately 0.95% [2]. Therefore, timely and appropriate intervention measures are required. Endovascular treatment has been proven to be a safe and effective method for treating IAs [3, 4]. Flow diverters (FDs), among the most commonly used stents, are designed to redirect blood flow away from the aneurysm sac and promote parent artery reconstruction, demonstrating a considerable advantage in treating large or giant wide-neck, fusiform, or complex aneurysms [5]. FDs have also become a mainstream strategy in clinical practice for small or medium-sized aneurysms [6, 7]. The safety and effectiveness of Tubridge in treating small and medium aneurysms have been well-documented [7, 8].

Unlike immediate embolization achieved through coiling, FDs exert a gradual effect on blood flow. Most aneurysms (up to 90.4%) occlude completely within 12 months, according to a previous study that enrolled 146 patients treated with Pipeline [9]. It is important to determine the reasons for persistent incomplete occlusion in some aneurysms even after 12 months of treatment. Several studies have identified key hemodynamic parameters as essential predictors of poor prognosis in treated aneurysms, such as a large inflow rate (Q_{inflow}) [10, 11], inflow with more localized and intense jet characteristics (large ICI) [12, 13], high velocity in the aneurysm sac [10, 14], and a large residual flow volume (RFV) [15, 16], prolonged residual time and low wall shear stress (WSS) [17]. Some morphological parameters may play important roles in the hemodynamic changes of FD treatment, such as the curvature of the parent artery and the morphology of the aneurysm neck [18–22]. Moreover, the outcomes of aneurysms of similar size but different locations vary significantly in clinical practice. The mechanism by which the morphological parameters of small aneurysms influence their hemodynamics after stenting remains unclear. Therefore, in this study, we selected patients with tandem aneurysms which had different prognoses after FD treatment to eliminate the effects of confounding factors. Virtual modifications were made to conduct controlled research into the relationship between aneurysm morphology and hemodynamics.

Results

Clinical performance and follow-up outcomes

A total of 12 patients with tandem aneurysms were treated with Tubridge during this period in our hospital. Among these, four patients were excluded due to incomplete imaging data (one patient lacked 3D-digital subtraction angiography images, and three patients lacked follow-up images). Additionally, three patients had incorporated branch arteries, one of whom was treated with coils; one patient had a giant aneurysm; one patient had two completely occluded aneurysms; one patient had two tandem aneurysms adhering to each other; and two patients had two small aneurysms with different outcomes. To compare the differences between occluded and remnant aneurysms, two patients with small aneurysms presenting different outcomes were selected for simulations. The coiled aneurysm in one of these patients was excluded from the analysis when obtaining variations.

Detailed information on the two patients is presented in Table 1. Patient 1 had three aneurysms, but the coiled aneurysms were excluded from this study. Of the two left-sided aneurysms, the aneurysm located on the superior wall (aneu2) was incompletely occluded after FD implantation for a year. As shown in Fig. 1, the remnant aneurysm appeared larger three months after treatment (B3 and B4) compared to its size before surgery (B1). Patient 2 also had an aneurysm located on the superior wall (aneu4) that persisted for approximately 3 years. Although this aneurysm decreased in size, it remained visible during the follow-up period, as illustrated in Fig. 2.

Hemodynamics of the practical plan

The clinical treatments applied to the two patients were simulated to identify differences between occluded and remnant aneurysms in hemodynamics. The postoperative results are depicted in Fig. 3, while the preoperative results are in Fig. S1 in Supplementary Material. Pre- and post-operative hemodynamic parameters, including Q_{inflow}, ICI, velocity in the sac and neck regions (v_{a} and v_{neck}), and RFV for velocities greater than 0.05 m/s, 0.1 m/s, 0.15 m/s, and 0.2 m/s were calculated. The incompletely occluded aneurysm (aneu2) exhibited larger v_{a} (0.182 m/s vs. 0.089.

(m/s), v_{neck} (0.200 m/s vs. 0.106 m/s), and relative RFV ($v > 0.05$ m/s: 72.47% vs. 55.31%; $v > 0.1$ m/s: 64.34% vs. 33.81%; $v > 0.15$ m/s: 53.63% vs. 11.34%; $v > 0.2$ m/s: 40.75% vs. 0.00%) than the occluded aneurysm (aneu1) in Patient 1 after treatment. Additionally, the two aneurysms of Patient 2 also showed differences in Q_{inflow} and ICI (Q_{inflow}: 0.973 mL/s (aneu4) vs. 0.102 mL/s (aneu3); ICI: 0.501 (aneu4) vs. 0.053 (aneu3)). All results are listed in Table 2

Table 1 Basic information of selected two patients

Characteristics	Patient 1		Patient 2	
Clinical information				
Gender	Male		Female	
Age	73		65	
Hypertension	No		Yes	
Diabetes	No		Yes	
Smoking	Yes		No	
Drinking	Yes		No	
FD size	Tubridge-4.5-25 mm		Tubridge-4.5-20 mm	
Aneurysm information	Aneu-1	Aneu-2	Aneu-3	Aneu-4
Neck width (mm)	4.7	3.9	4.1	4.9
Height (mm)	1.8	1.0	1.5	4.0
Location	C6	C6	C6	C6
Relative location to parent artery	Inferior	Superior	Inferior	Superior
Follow-up at 3 months	Remnant	Remnant	Occluded	Remnant
Follow-up at 6 months	–	–	Occluded	Remnant
Follow-up at 12 months	Occluded	Remnant	–	–
Follow-up over 2 years	–	–	Occluded	Remnant

FD flow diverter

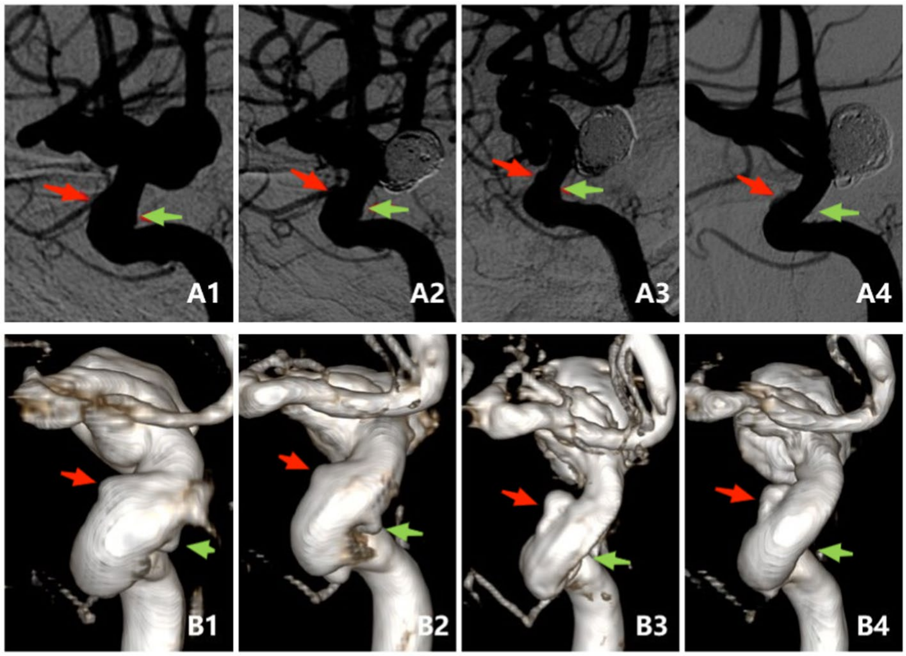

Fig. 1 DSA imaging of patient 1. A1–A4 were 2D-DSA images of pre-, post-operation, and follow-up for 3 and 12 months. B1–B4 were 3D volume-rendering models of pre-, post-operation, and follow-up for 3 and 12 months. The small aneurysm at the superior wall of the internal carotid artery (red arrow) demonstrated progressive enlargement during follow-up, whereas the inferior wall aneurysm (green arrow) showed complete occlusion at both 3- and 12-month follow-up evaluations

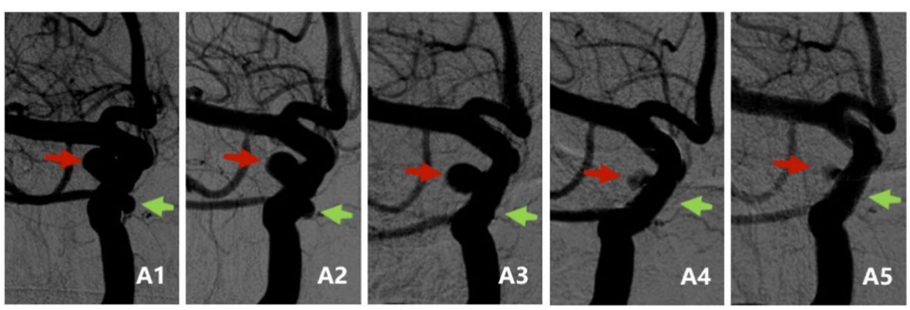

Fig. 2 DSA imaging of patient 2. A1–A5 were 2D-DSA images of pre-, post-operation, and follow-up for 3, 6 and 35 months. The small aneurysm at the superior wall of the internal carotid artery (red arrow) exhibited an occlusion tendency but demonstrated persistent filling, while the inferior wall aneurysm (green arrow) showed complete occlusion at the 3-month follow-up evaluation

Hemodynamics of the variations

A total of 28 aneurysms, comprising four initial and 24 modified variants, were analyzed. Similarly, Q_{inflow}, ICI, v_{neck}, v_{a}, and RFV were calculated to study the effects of aneurysm neck width and height on hemodynamics. The trend of hemodynamic parameters changing with width and height are presented in Figs. 4 and 5, respectively. The sets of incompletely occluded aneurysms are depicted by red lines marked with squares and inverted triangles. A1–A4 represent aneu1–aneu4 and their variants, respectively.

As neck width increased, Q_{inflow}, ICI, v_{a}, and relative RFV also increased. For Q_{inflow} and ICI, aneurysms located on the superior wall in Patient 2 (A4) were most sensitive

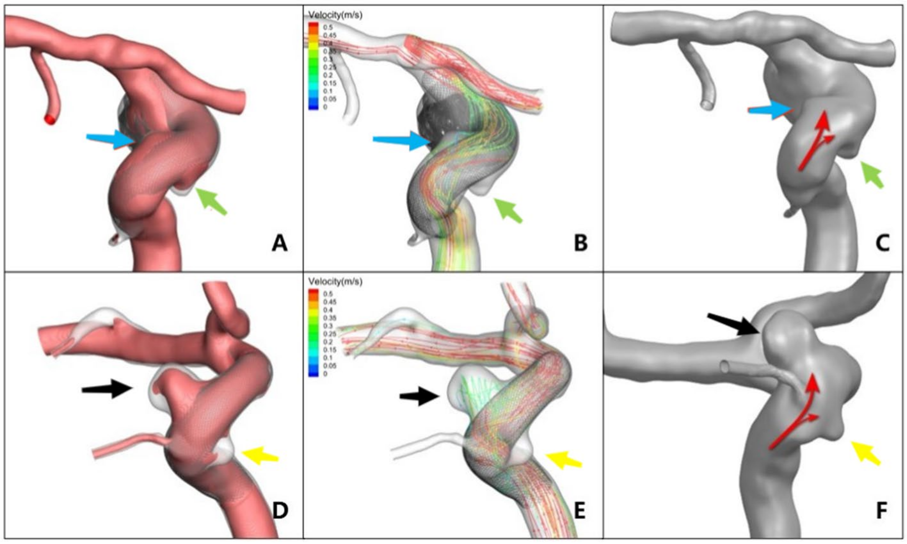

Fig. 3 Visualized results and aneurysm models of two patients. A/B (D/E) were volume of velocity greater than 0.1 m/s and the streamline of patient 1 (patient 2). C/F were initial aneurysm models and red arrows represented blood flowing into the aneurysm sac. The thickness of the arrows represented the impact strength of blood on the aneurysm. Blue and green arrows represented a small aneurysm at the superior and inferior wall of the internal carotid artery of patient 1. Black and yellow arrows represented a small aneurysm at the superior and inferior wall of the internal carotid artery of patient 2

Table 2 Hemodynamic results of actual treatment plan for two patients

Parameters		Aneu-1		Aneu-2		Aneu-3		Aneu-4	
		Pre	Post	Pre	Post	Pre	Post	Pre	Post
Q_{inflow} (mL/s)		0.448	0.187	0.281	0.174	0.336	0.102	1.263	0.973
ICI		0.232	0.108	0.143	0.087	0.155	0.053	0.643	0.501
v_a (m/s)		0.223	0.089	0.270	0.182	0.181	0.078	0.325	0.174
v_{neck} (m/s)		0.245	0.106	0.287	0.200	0.301	0.129	0.336	0.184
RFV (mm [3])	$v > 0.05$ m/s	3.612	2.920	2.653	3.548	2.765	2.305	39.873	40.206
	$v > 0.1$ m/s	3.439	1.785	2.632	3.150	2.322	1.349	39.598	36.895
	$v > 0.15$ m/s	3.123	0.599	2.558	2.626	1.978	0.460	38.647	31.580
	$v > 0.2$ m/s	2.517	0	2.377	1.995	1.638	0.009	36.929	17.319
Relative RFV	$v > 0.05$ m/s	60.8%	55.3%	60.4%	72.5%	72.5%	62.1%	89.8%	90.5%
	$v > 0.1$ m/s	57.9%	33.8%	59.9%	64.3%	60.9%	36.4%	89.2%	83.0%
	$v > 0.15$ m/s	52.6%	11.3%	58.2%	53.6%	51.9%	12.4%	87.1%	71.1%
	$v > 0.2$ m/s	42.4%	0	54.1%	40.8%	42.9%	0.25%	83.2%	39.0%

Q_{inflow} inflow rate at the neck, *ICI* inflow concentration index, v_a and v_{neck} blood velocity of the sac and neck, *RFV* volume of velocity greater than 0.05 m/s, 0.1 m/s, 0.15 m/s and 0.2 m/s, respectively. Relative RFV: the ratio of RFV to volume of aneurysm.

to changes in neck width, whereas other aneurysms (A1, A2, and A3) showed similar but slower growth. The velocity in the aneurysm sac increased with the neck width, and the two red lines (A2 and A4) showed steeper slopes than those of the two black lines (A1 and A3). The influence of neck width on v_{neck} was different, as shown in Fig. 4. The lines for A1 and A3 remained nearly stable; the line for A4 first decreased and then flattened, whereas the line for A2 continued to increase, showing a more

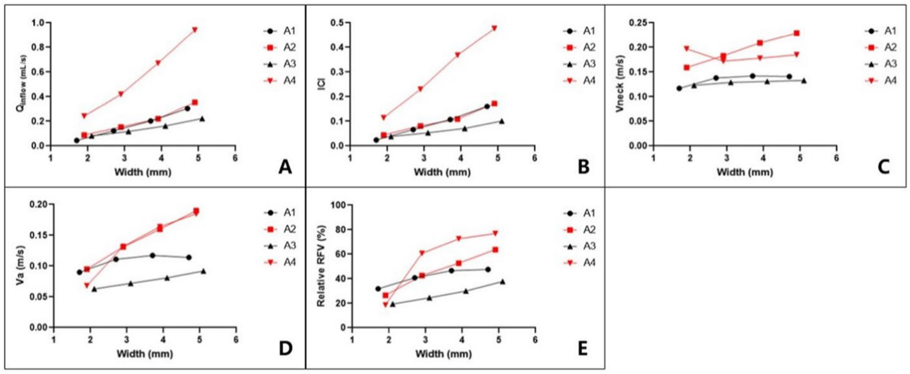

Fig. 4 The influence of neck width to Q_{inflow}, ICI, v_{neck}, v_{a}, and RFV of velocity greater than 0.1 m/s

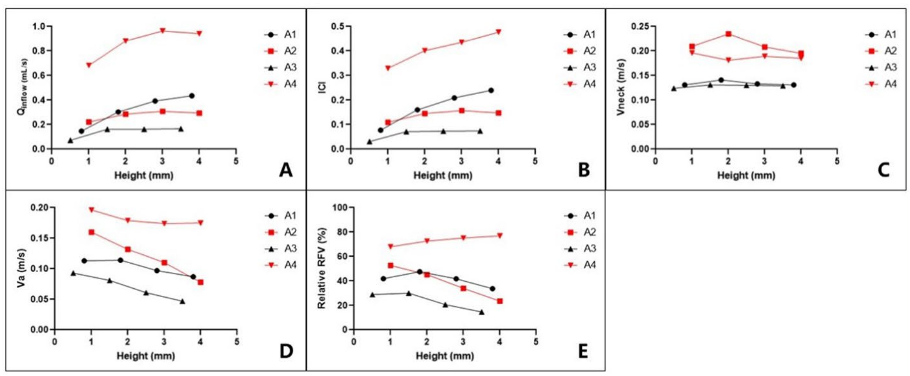

Fig. 5 The influence of height on Q_{inflow}, ICI, v_{neck}, v_{a}, and RFV of velocity greater than 0.1 m/s

pronounced rise. Interestingly, the two red lines consistently remained above the black lines.

Figure 5 shows the variations in hemodynamics resulting from changes in height with a constant neck width. As height increased, Q_{inflow} and ICI exhibited trends similar to those observed with neck width; however, the lines leveled off when the height exceeded 2 mm. Conversely, unlike the effect of neck width, v_{a} and relative RFV decreased with increasing height, except for the relative RFV of A4. The V_{neck} of A1 and A3 (black lines) was minimally affected by increases in height. However, similar to the trends shown in Fig. 4C, the red lines overtook the black lines, showing slight fluctuations around a height of 2 mm.

Discussion

Hemodynamics plays an important role in the poor prognosis of IAs (delayed occlusion, regrowth, or rupture). The design of FDs changes the treatment concept for aneurysms, shifting from rapid, dense embolization of the sac to slow, thrombosed occlusion by reconstructing the parent artery and inducing endothelial growth on the stent surface [23]. This study investigated changes in several hemodynamic parameters associated with poor outcomes, driven by increases in neck width or height, based on two cases of tandem aneurysms with different outcomes. Aneurysms with larger neck width or height (volume) exhibited a larger flow rate, and the two incompletely occluded aneurysms and their variants had a larger v_{neck} compared with that of the other two groups.

One interesting finding of this study was that the velocity at the neck of aneurysms in A2 and A4 was greater than that in the other two sets, as shown in Figs. 4C and 5C. A2 and A4 represent two sets of aneurysms derived from two remnant aneurysms located on the superior wall of the ophthalmic segment of the ICA. Because of the curvature of the ICA, aneurysms located on the superior wall are more prone to being impacted by blood flowing through the bend than those on the inferior wall (Fig. 3C and F). Consequently, higher-velocity blood is more likely to flow toward the sac of superior aneurysms, increasing the risk of rupture in untreated cases. Similar studies have explored the relationship between aneurysm orientation and blood flow direction [24–26]. For instance, Dhar et al. [24] and Duan et al. [25] identified aneurysm angle and flow angle as risk factors for rupture. Additionally, a review of the literature highlighted that the direction of the aneurysm dome is a risk factor for the rupture of anterior communicating artery aneurysms [26]. However, the relationship between delayed occlusion after FD treatment and aneurysm direction has not yet been reported. Considering the mechanism of FD treatment, FDs promote endothelialization on the stent surface and facilitate thrombus formation to achieve aneurysm occlusion [27]. However, high-velocity flow with elevated wall shear stress (WSS) may inhibit neointimal growth [28]. The results of this study, which show incomplete occlusion and elevated v_{neck} in superior aneurysms, provide evidence supporting this hypothesis. Thus, further studies with larger case numbers are needed to quantify the relationship between aneurysm orientation and blood flow dynamics, which may help explain delayed occlusion.

Neck size (width or diameter) and derived parameters, such as the aspect ratio (the ratio of height to neck width), have already been reported as risk factors for rupture [29–31]. A significant difference in neck width between remnant and completely occluded aneurysms was reported in Yang's study [32]. All these studies demonstrated that aneurysms with large necks tend to have more complex flow patterns, often resulting in poor outcomes. However, it remains unclear which hemodynamic parameters are most affected by an enlarged neck and how they contribute to delayed occlusion. This study provides insights into these questions. With an increase in neck width, Q_{inflow}, ICI, v_{a}, and RFV increased across all sets of variants. Large Q_{inflow} and ICI values indicate that strong and locally impacting blood continues to flow into the aneurysm sac, even after FD implantation, adversely affecting the endothelial process. Moreover, occlusion of the aneurysm dome is strongly associated with slow-flow-induced thrombosis [33], and high velocity (v_{a} or RFV) can inhibit this process.

Aneurysm height is frequently measured and evaluated in aneurysm studies [25, 34, 35]. Perpendicular height [34] and changes in height [35] have been identified as risk factors for rupture. The size ratio (the ratio of aneurysm height to parent artery diameter), a predictive factor for the rupture of small aneurysms [25, 36], showed a similar effect on hemodynamics in this study because of the consistent parent artery geometry. However, the simulations and statistical analyses in these studies were conducted on different patient samples, and confounding factors could not be fully controlled. According to the results of this study, the growth of Q_{inflow} and ICI was limited as height increased.

This implies that the effect of height on altering blood flow state is restricted when other factors remain constant. In clinical practice, we have observed that some aneurysms exhibit significant occlusion near the dome in the short term after treatment, yet complete occlusion remains unachieved despite years of follow-up. One possible explanation is that the necks of these aneurysms were not fully treated during surgery. During the occlusion process, the thrombus formation at the aneurysm dome progressed smoothly with notable height reduction, while hemodynamic improvements in the neck region were limited, preventing complete occlusion. Therefore, aneurysm neck width may exert a more significant influence on postoperative thrombus formation than aneurysm height.

Our center prioritizes the use of FD combined with loose coiling for treating superior wall of ICA aneurysms, with coils primarily deployed in the inflow zone and aneurysm neck. For such lesions, we recommend preoperative CFD evaluation. However, due to the limited sample size, further expansion of the sample size is required to explore hemodynamic parameter thresholds associated with superior wall aneurysm occlusion.

This study had several limitations. First, the analysis of 28 models derived from four aneurysms in two patients provides only trends in variation and lacks statistical significance. Based on the trend obtained from this study, the patient screening criteria can be relaxed to explore statistical significance in a larger case set. Second, the variation range of independent variables was relatively small (neck width ranged from 1.7 to 5.1 mm; height ranged from 0.5 to 4.0 mm) because of the small size of the initial aneurysms. Finally, certain assumptions were adopted to simplify calculations in the CFD simulations, such as inlets and outlets condition, and properties of the vessel wall and blood. Previous studies have discussed the impact of hypotheses on computational results [37–40]. The Newtonian fluid hypothesis may overestimate the flow velocity in high shear rate regions, while the rigid wall hypothesis may overestimate the flow velocity and pressure. The assumed inlet flow may weaken the individualized differences between patients. However, simplified analysis has improved the feasibility of conducting simulation research and has been adopted by many teams.

Conclusion

Aneurysms located on the superior wall of the ICA ophthalmic segment exhibit higher neck velocities compared to those on the inferior wall. Additionally, aneurysms with large volumes (large neck or height) present a more severe hemodynamic environment, necessitating greater consideration during surgical planning. This study provides hemodynamic evidence supporting the influence of morphology on aneurysm progression.

Methods

Study design

To investigate whether the volume and location of aneurysms affect hemodynamics and lead to different clinical outcomes, this study was conducted from two perspectives. First, we collected cases with tandem aneurysms which had different prognoses after FD treatment, simulated the preoperative and postoperative hemodynamics of the actual treatment plan, and evaluated the calculated results in conjunction with the clinical outcomes. Tandem aneurysms were selected to exclude interference from other baseline information and explore the relation between aneurysm morphology and hemodynamics. Second, all selected tandem aneurysms were separated from each other to make a single aneurysm the research object. Variations in each aneurysm were obtained through idealized operations to study the influence of a single morphological parameter on hemodynamics.

Patient selection and simulation analysis

The study was approved by the Shanghai Jing'an District Central Hospital Medical Ethics Committee. Informed consent was exempted for retrospective study. Patients with internal carotid artery (ICA) aneurysms admitted to our hospital between August 2020 and December 2023 who underwent treatment with a Tubridge FD (MicroPort, China) were enrolled in this study. The inclusion criteria were as follows: (1) patients with small or medium tandem (< 10 mm) aneurysms treated with Tubridge alone; (2) complete imaging data to reconstruct the complete vessel model; and (3) patients with multiple follow-up imaging studies. The exclusion criteria were as follows: (1) fusiform or dissecting aneurysms; (2) aneurysms incorporated into a branch artery; and (3) tandem aneurysms adhering to each other.

Patient-specific aneurysm models were reconstructed based on preoperative 3D digital subtraction angiography images. Finite element simulations for FD stent deployment and computational fluid dynamics (CFD) computed fluid dynamics simulations were performed using AneuPlan (ArteryFlow Technology, China), adopting the methods of previous studies [41]. A population-based pulsatile inflow with an average of 4.6 mL/s was set as the inlet boundary condition and the boundary condition of outlets were based on Murray's law with a cube exponent.

The calculated hemodynamic parameters include the inflow rate at the neck (Q_{inflow}), ICI, the average velocity of the aneurysm sac (V_{a}), and the relative RFV in the aneurysm sac. The relative RFV was the proportion of the area with a flow velocity greater than 0.1 in the aneurysm lumen to the volume of the aneurysm. The calculation formula for ICI is

$$\text{ICI} = \frac{Q_{inflow}/Q_v}{A_{in}/A_0}$$

where Q_{v} is the flow rate in the parent artery, A_{in} is the area of the inflow region, and A_{o} is the area of the ostium surface.

Variations and simulation analysis

To investigate the influence of volume and location on hemodynamics, some variations in aneurysms were obtained using Geomagic Wrap 2015 (Research Triangle Park, North Carolina, United States). Compared to volume, the neck width and height of the aneurysm were more distinct and convenient to measure using the 3D volume-rendering model obtained from the angiography device before surgery. Therefore, the neck width and height of the aneurysm served as two independent variables representing the change in volume in this study.

Tandem aneurysms eliminate the influence of factors other than the aneurysm itself. However, in this section, we aim to study how aneurysm morphology affects the hemodynamic parameters related to delayed occlusion after treatment with an FD. Therefore, selected tandem aneurysms were classified into different models. Each aneurysm treated with an FD alone was a single object, whereas the other aneurysms were removed and replaced with a healthy vessel wall. Furthermore, the neck width and height were varied to determine the influence of a single factor on aneurysm hemodynamics. Operations focused on the neck width of the aneurysm were performed in 1 mm increments or decrements, and this process was repeated three times to obtain three inflated or deflated variations in the neck width. All operations were performed using the offset function in Geomagic Wrap 2015, which raised or lowered a selected set of polygons by a given distance in the normal direction and created additional triangles to maintain a complete overall surface. To obtain a set of aneurysms with the same height but different neck widths, the bottom region of the aneurysm was selected. All these processes were repeated to obtain variations at different heights. For each aneurysm, there were seven models, including six variations (three variations in neck width and three variations in height) and one initial model. The samples are displayed in Fig. 6. All the aforementioned aneurysm models were also subjected to finite element and CFD simulations.

Basic information.

Hypertension was defined as a confirmed office systolic BP of ≥ 140 mmHg or diastolic BP of ≥ 90 mmHg according to the 2024 Guidelines [42].

Criteria for the diagnosis of diabetes(type 2) in nonpregnant individuals [43]: haemoglobin A1c(HbA1c) > 6.5% (48 mmol/mol), OR fasting plasma glucose(FPG) > 7.0 mmol/L (126 mg/dL), OR 2 h plasma glucose(2hPG) > 11.1 mmol/L (> 200 mg/dL).

The World Health Organization (WHO) defines a smoking history as smoking ≥ 1 cigarette per day for a duration exceeding 6 months.

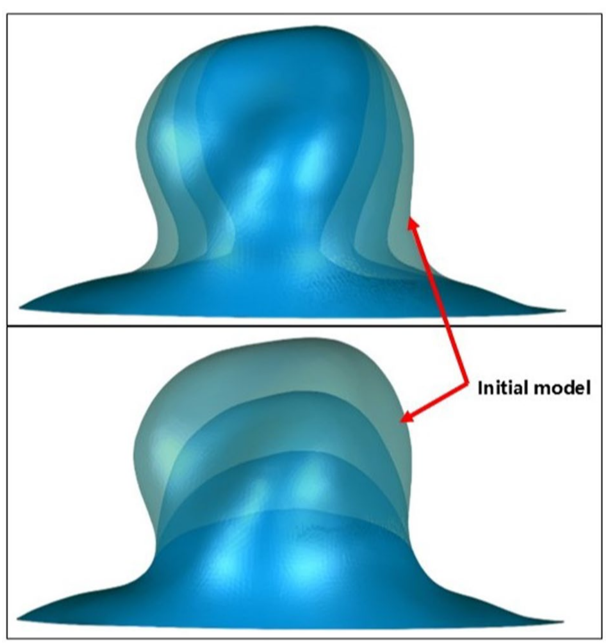

Fig. 6 A sample of variations for an aneurysm. The top picture presents variations focused on the neck width, and the bottom picture presents variations focused on the height

The WHO defines an alcohol consumption history as drinking alcohol ≥ 1 time per week, with a cumulative alcohol intake equivalent to ≥ 50 mL of pure alcohol per week, lasting for more than 6 months.

Supplementary Information

The online version contains supplementary material available at https://doi.org/10.1186/s12938-025-01379-4.

Additional file 1.

Author contributions

S W and X Z conceived and designed the research. L X and Y J acquired the data. Q Z and G X analyzed and interpreted the data. L Y and X L performed hemodynamic simulation and analysis. L X and Y J performed the statistical analysis. S W and X Z performed the supervision. J W drafted the manuscript.

Funding

This study was unfunded.

Data availability

Data is provided within the manuscript.

Declarations

Ethics approval and consent to participate

All procedures performed in studies involving human participants were in accordance with the ethical standards of the institutional and/or national research committee and with the 1964 Helsinki declaration and its later amendments or comparable ethical standards. For this type of study formal consent is not required.

Consent for publication

Informed consent was obtained from all individual participants included in the study.

Competing interests

The authors declare that we have no conflict of interest.

Received: 22 January 2025 Accepted: 2 April 2025
Published online: 12 April 2025

References

1. Lv B, Lan JX, Si YF, Ren YF, Li MY, Guo FF, et al. Epidemiological trends of subarachnoid hemorrhage at global, regional, and national level: a trend analysis study from 1990 to 2021. Mil Med Res. 2024;11:46. https://doi.org/10.1186/s40779-024-00551-6.
2. Chalouhi N, Hoh BL, Hasan D. Review of cerebral aneurysm formation, growth, and rupture. Stroke. 2013;44:3613–22. https://doi.org/10.1161/STROKEAHA.113.002390.
3. Wiebers DO, Whisnant JP, Huston JR, Meissner I, Brown RJ, Piepgras DG, et al. Unruptured intracranial aneurysms: natural history, clinical outcome, and risks of surgical and endovascular treatment. Lancet. 2003;362:103–10. https://doi.org/10.1016/s0140-6736(03)13860-3.
4. Molyneux AJ, Birks J, Clarke A, Sneade M, Kerr RS. The durability of endovascular coiling versus neurosurgical clipping of ruptured cerebral aneurysms: 18 year follow-up of the UK cohort of the international subarachnoid aneurysm trial (ISAT). Lancet. 2015;385:691–7. https://doi.org/10.1016/S0140-6736(14)60975-2.
5. Kallmes DF, Brinjikji W, Cekirge S, Fiorella D, Hanel RA, Jabbour P, et al. Safety and efficacy of the Pipeline embolization device for treatment of intracranial aneurysms: a pooled analysis of 3 large studies. J Neurosurg. 2017;127:775–80. https://doi.org/10.3171/201-6.8.JNS16467.
6. Arai S, Fujii T, Teranishi K, Nonaka S, Kitamura T, Mitome-Mishima Y, et al. Pipeline flex with shield technology placement for small- and medium-sized aneurysms achieves early complete occlusion. Neurol Med Chir. 2023;63:58–64. https://doi.org/10.2176/jns-nmc.2022-0217.
7. Xie D, Yang H, Zhao L, Ye X, Yang S, Gao C, et al. Tubridge flow diverter for the treatment of small and medium aneurysms. Front Neurol. 2023;14:1054631. https://doi.org/10.3389/fn-eur.2023.1054631.
8. Li L, Shao QJ, Li TX, Wang ZL, Zhang K, Gao BL. Effect and safety of tubridge flow diverter in the treatment of unruptured intracranial aneurysms. Medicine. 2022;101: e31672. https://doi.org/10.1097/-MD.0000000000031672.
9. Chalouhi N, Patel PD, Atallah E, Starke RM, Chitale A, Lang M, et al. Low yield of cerebral angiography in adequately occluded aneurysms after flow diversion. Neurosurgery. 2018;83:1294–7. https://doi.org/10.1093/neuros/nyx625.
10. Mut F, Raschi M, Scrivano E, Bleise C, Chudyk J, Ceratto R, et al. Association between hemodynamic conditions and occlusion times after flow diversion in cerebral aneurysms. J NeuroInterv Surg. 2015;7:286–90. https://doi.org/10.1136/neurintsurg-2013-011080.

11. Su T, Reymond P, Brina O, Bouillot P, Machi P, Delattre B, et al. Large neck and strong ostium inflow as the potential causes for delayed occlusion of unruptured sidewall intracranial aneurysms treated by flow diverter. Am J Neuroradiol. 2020;41:488–94.
12. Cebral JR, Mut F, Weir J, Putman C. Quantitative characterization of the hemodynamic environment in ruptured and unruptured brain aneurysms. AJNR Am J Neuroradiol. 2011;32:145–51. https://doi.org/10.3174/ajnr.A2419.
13. Chung BJ, Doddasomayajula R, Mut F, Detmer F, Pritz MB, Hamzei-Sichani F, et al. Angioarchitectures and hemodynamic characteristics of posterior communicating artery aneurysms and their association with rupture status. AJNR Am J Neuroradiol. 2017;38:2111–8. https://doi.org/10.3174/ajnr.A5358.
14. Kulcsár Z, Augsburger L, Reymond P, Pereira VM, Hirsch S, Mallik AS, et al. Flow diversion treatment: intra-aneurismal blood flow velocity and WSS reduction are parameters to predict aneurysm thrombosis. Acta Neurochir. 2012;154:1827–34. https://doi.org/10.1007/s00701-012-1482-2.
15. Umeda Y, Ishida F, Tsuji M, Furukawa K, Shiba M, Yasuda R, et al. Computational fluid dynamics (CFD) using porous media modeling predicts recurrence after coiling of cerebral aneurysms. PLoS ONE. 2017;12: e0190222. https://doi.org/10.1371/journal.pone.0190222.
16. Beppu M, Tsuji M, Ishida F, Shirakawa M, Suzuki H, Yoshimura S. Computational fluid dynamics using a porous media setting predicts outcome after flow-diverter treatment. Am J Neuroradiol. 2020;41:2107–13. https://doi.org/10.3174/ajnr.A6766.
17. Rayz VL, Boussel L, Ge L, Leach JR, Martin AJ, Lawton MT, McCulloch C, Saloner D. Flow residence time and regions of intraluminal thrombus deposition in intracranial aneurysms. Ann Biomed Eng. 2010;38:3058–69. https://doi.org/10.1007/s10439-010-0065-8.
18. Larrabide I, Geers AJ, Morales HG, Aguilar ML, Rüfenacht DA. Effect of aneurysm and ICA morphology on hemodynamics before and after flow diverter treatment. J NeuroInterv Surg. 2015;7:272–80. https://doi.org/10.1136/neurintsurg-2014-011171.
19. Chong W, Zhang Y, Qian Y, Lai L, Parker G, Mitchell K. Computational hemodynamics analysis of intracranial aneurysms treated with flow diverters: correlation with clinical outcomes. Am J Neuroradiol. 2014;35:136–42. https://doi.org/10.3174/ajnr.A3790.
20. Paliwal N, Tutino VM, Shallwani H, Beecher JS, Damiano RJ, et al. Ostium ratio and neck ratio could predict the outcome of sidewall intracranial aneurysms treated with flow diverters. Am J Neuroradiol. 2019;40:288–94. https://doi.org/10.3174/ajnr.A5953.
21. Damiano RJ, Tutino VM, Paliwal N, Patel TR, Waqas M, Levy EI, et al. Aneurysm characteristics, coil packing, and post-coiling hemodynamics affect long-term treatment outcome. J NeuroInterv Surg. 2020;12:706–13. https://doi.org/10.1136/neurintsurg-2019-015422.
22. Neki H, Kohyama S, Otsuka T, Yonezawa A, Ishihara S, Yamane F. Optimal first coil selection to avoid aneurysmal recanalization in endovascular intracranial aneurysmal coiling. J NeuroInterv Surg. 2018;10:50–4. https://doi.org/10.1136/neurintsurg-2016-012877.
23. Kadirvel R, Ding YH, Dai D, Rezek I, Lewis DA, Kallmes DF. Cellular mechanisms of aneurysm occlusion after treatment with a flow diverter. Radiology. 2014;270:394–9. https://doi.org/10.1148/rad-iol.13130796.
24. Dhar S, Tremmel M, Mocco J, Kim M, Yamamoto J, Siddiqui AH, et al. Morphology parameters for intracranial aneurysm rupture risk assessment. Neurosurgery. 2008;63:185–97. https://doi.org/10.1227/-01.NEU.0000316847.64140.81.
25. Duan Z, Li Y, Guan S, Ma C, Han Y, Ren X, et al. Morphological parameters and anatomical locations associated with rupture status of small intracranial aneurysms. Sci Rep. 2018;8:6440. https://doi.org/10.1038/s41598-018-24732-1.
26. Cai W, Hu C, Gong J, Lan Q. Anterior communicating artery aneurysm morphology and the risk of rupture. World Neurosurg. 2018;109:119–26. https://doi.org/10.1016/-j.wneu.2017.09.118.
27. Alderazi YJ, Shastri D, Kass-Hout T, Prestigiacomo CJ, Gandhi CD. Flow diverters for intracranial aneurysms. Stroke Res Treat. 2014;2014: 415653. https://doi.org/10.1155/2014/415653.
28. Akimoto SMM, Sasaguri T, Yoshida Y. Laminar shear stress inhibits vascular endothelial cell proliferation by inducing cyclin-dependent kinase inhibitor p21(Sdi1/Cip1/Waf1). Circ Res. 2000;86:185–90. https://doi.org/10.1161/01.res.86.2.185.
29. Kocur D, Przybylko N, Niedbala M, Rudnik A. Alternative definitions of cerebral aneurysm morphologic parameters have an impact on rupture risk determination. World Neurosurg. 2019;126:e157–64. https://doi.org/10.1016/j.wneu.2019.01.283.
30. Qiu TL, Jin GL, Bao WQ, Lu HT. Morphological effect on wall shear stress in intracranial aneurysms. J Neurol Surg A Cent Eur Neurosurg. 2018;79:108–15. https://doi.org/10.1055/s-0037-1603634.
31. Xu WD, Wang H, Wu Q, Wen LL, You ZQ, Yuan B, et al. Morphology parameters for rupture in middle cerebral artery mirror aneurysms. J Neurointerv Surg. 2020;12:858–61. https://doi.org/10.1136/-neurintsurg-2019-015620.
32. Yang SH, Hampton T, Kandasamy N, Hart J, Ashmore J, Walsh DC, et al. Outcome study of the pipeline embolization device for treatment of intracranial aneurysms at a single UK institution. Br J Neurosurg. 2017;31:661–7. https://doi.org/10.1080/02688697.2017.1354121.
33. Cebral JR, Mut F, Raschi M, Hodis S, Ding YH, Erickson BJ, et al. Analysis of hemodynamics and aneurysm occlusion after flow-diverting treatment in rabbit models. Am J Neuroradiol. 2014;35:1567–73. https://doi.org/10.3174/ajnr.A3913.
34. Mocco J, Brown RJ, Torner JC, Capuano AW, Fargen KM, Raghavan ML, et al. Aneurysm morphology and prediction of rupture: an international study of unruptured intracranial aneurysms analysis. Neurosurgery. 2018;82:491–6. https://doi.org/10.1093/neuros/nyx226.
35. Wang B, Shen C, Su Z, Nie X, Zhao J, Qiu S, et al. Correlation between the rate of morphological changes and rupture of intracranial aneurysms during one cardiac cycle analyzed by 4D-CTA. Front Neurol. 2023;14:1235312. https://doi.org/10.3389/fneur.2023.1235312.
36. Kashiwazaki D, Kuroda S. Size ratio can highly predict rupture risk in intracranial small (<5 mm) aneurysms. Stroke. 2013;44:2169–73. https://doi.org/10.1161/STROKEA-HA.113.001138.

37. Xiang J, Tremmel M, Kolega J, Levy EI, Natarajan SK, Meng H. Newtonian viscosity model could overestimate wall shear stress in intracranial aneurysm domes and underestimate rupture risk. J NeuroInterv Surg. 2012;4:351–7. https://doi.org/10.1136/neurintsurg-2011-010089.
38. Najafi M, Cancelliere NM, Brina O, Bouillot P, Vargas MI, Delattre BMA, Pereira VM, Steinman DA. How patient-specific do internal carotid artery inflow rates need to be for computational fluid dynamics of cerebral aneurysms? J NeuroInterv Surg. 2021;13:459–64. https://doi.org/10.1136/neurintsurg-2020-015993.
39. Berg P, Roloff C, Beuing O, Voss S, Sugiyama S-I, Aristokleous N, Anayiotos AS, Ashton N, Revell A, Bressloff NW, et al. The computational fluid dynamics rupture challenge 2013—phase ii: variability of hemodynamic simulations in two intracranial aneurysms. J Biomech Eng. 2015. https://doi.org/10.1115/1.4031794.
40. Janiga G, Berg P, Sugiyama S, Kono K, Steinman DA. The computational fluid dynamics rupture challenge 2013—Phase I: prediction of rupture status in intracranial aneurysms. Am J Neuroradiol. 2015;36:530–6. https://doi.org/10.3174/ajnr.A4157.
41. Wang M, Shi S-N, Xiang J-P, Wan S. Establishing surgical plan of endovascular intervention for intracranial aneurysm using AneuPlan™—an exploratory study. Asian J Surg. 2024;47:5191–3. https://doi.org/10.1016/j.asjsur.2024.05.273.
42. McEvoy JW, McCarthy CP, Bruno RM, Brouwers S, Canavan MD, Ceconi C, et al. ESC Guidelines for the management of elevated blood pressure and hypertension. Eur Heart J. 2024;45(38):3912–4018. https://doi.org/10.1093/eurheartj/ehae178.
43. Cosentino F, Grant PJ, Aboyans V, Bailey CJ, Ceriello A, Delgado V, et al. ESC Guidelines on diabetes, pre-diabetes, and cardiovascular diseases developed in collaboration with the EASD. Eur Heart J. 2020;41(2):255–323. https://doi.org/10.1093/eurheartj/ehz486.

Publisher's Note